
183rd Meeting of the Acoustical Society of America

Nashville, Tennessee

5-9 December 2022

Noise: Paper 4pNS3

Implementing a heuristic method to correct ground reflection effects observed in full-scale tactical aircraft noise measurements

Matthew A. Christian

*Department of Mechanical Engineering, Brigham Young University, Provo, UT, 84604;
mattachristian66@gmail.com*

Kent L. Gee and Jacob B. Streeter

*Department of Physics and Astronomy, Brigham Young University, Provo, UT, 84604;
kentgee@byu.edu; jacobbstreeter@gmail.com*

Alan T. Wall

Air Force Research Laboratory, Wright-Patterson AFB, OH, 45433; alan.wall.4@us.af.mil

Steven C. Campbell

*Ball Aerospace: Ball Aerospace and Technologies Corp., Dayton, OH, 45433;
steven.campbell.28.ctr@us.af.mil*

In a recent study of noise from a T-7A-installed GE F404 engine, microphones along a 76 m (250 ft) arc were mounted 1.8 m (5 ft) above the ground to quantify human impacts. While helpful for this purpose, the resulting multipath effects pose challenges for other acoustical analyses. For jet noise runup measurements, these effects are complicated by the fact that the noise source is extended and partially correlated, and its spatial properties are frequency dependent. Furthermore, a finite-impedance ground surface and atmospheric turbulence affect interference nulls. This study applies a ground-reflection method developed previously [Gee *et al.*, Proc. Mtgs. Acoust. **22**, 040001 (2014)] for rocket noise measurements. The model accounts for finite ground impedance, atmospheric turbulence, and extended source models that are treated as coherent and incoherent arrays of monopoles. Application to the ground runup data to correct the 76 m spectra at a range of angles suggests the incoherent line source model is more appropriate at upstream and sideline angles whereas the coherent source model is more appropriate for downstream propagation. Comparisons with near-field data and similarity spectra show that, while imperfect, this method represents an advancement in correcting jet noise spectra for ground reflection effects.

1. INTRODUCTION

The measurement of noise from full-scale afterburning jet engines presents unique challenges relative to other jet noise studies. The size and power of military-style jet engines all but require that any measurement take place outdoors, where factors such as atmospheric turbulence and ground reflections can significantly affect spectral and overall measured noise characteristics. Accounting for these parameters is an important step in developing physics-based models that characterize jet noise. Daigle¹ developed a model that accounts for both the effects of a finite-impedance ground as well as a turbulent atmosphere on the spectrum of a simple source. While other, more complicated, models do exist, Salomons et al.² showed that this Daigle model was adequate for most applications. Gee et al.³ improved upon the Daigle model by allowing for the inclusion of an extended source.

In far-field data recently measured from a T-7A-installed GE F404 engine, nulls attributed to ground reflections are observed in the spectra at or near the peak frequency at several of the measured angles. In this paper, the model developed by Gee et al.³ is applied to the T-7A far-field data to account for ground reflection effects. Though briefly mentioned in Christian et al.⁴, this paper represents a more in-depth description of the first implementation of this model into a full-scale supersonic jet noise study.

2. DATA COLLECTION

In August 2019, the Air Force Research Laboratory (AFRL) led a multi-organizational effort in measuring the noise from an F404-GE-103 engine installed in the new Boeing/Saab T-7A “Red Hawk.” The measurement, which took place at Holloman Air Force Base, New Mexico, consisted of over 200 microphones arranged in the near and far-fields. During the measurement, the aircraft was tied down to the run-up pad and was run at seven distinct engine conditions from idle to afterburner (AB) for 30 seconds each. This paper only uses data from the four most powerful engine conditions, 82% N2, 88% N2, military power (MIL), and AB. Of the considered engine powers, the fully expanded jet velocity was found to be subsonic at 82% N2, slightly supersonic at 88% N2, and well within the supersonic regime at MIL and AB.

All microphones were arranged relative to the microphone array reference point (MARP), which was located 4.0 m (13 ft) downstream of the aircraft nozzle. The microphones used for this paper were arranged along a 76 m (250 ft) arc from 30° to 160°, as shown in Fig. 1. The arc consisted of 22 1/4” GRAS 46 BD microphones connected via InfiniBand and BNC cables to NI PXI-4496 cards installed in an NI PXIe-1062Q chassis. Due to a loose connection, data from the 130° microphone were corrupted and will not be included here. The far-field microphones were mounted on tripods 1.5 m (5 ft) above the ground to study human impact. Additional information regarding this measurement can be found in Leete et al.⁵.

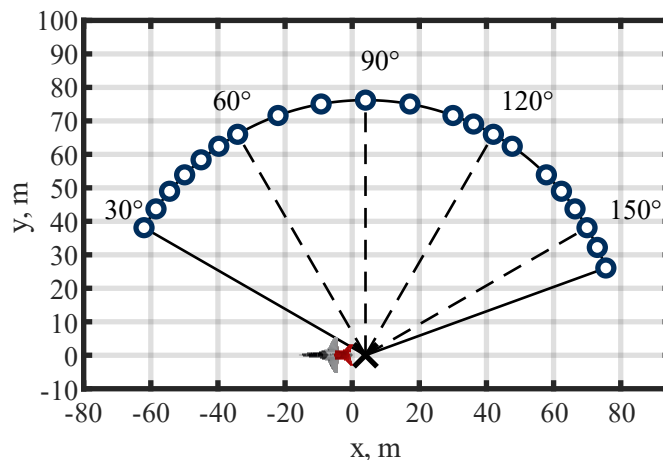


Figure 1: Diagram of the 78 m (250 ft) microphone arc arranged relative to the MARP, shown as an “X” behind the aircraft.

Though the aircraft was run-up six times, only data collected during the last four run-ups are used here. The first two run-ups are omitted due to changes in spectral nulls attributed to changes in the temperature gradient as

the sun rose. Figure 2 shows the approximate microphone locations superimposed on a satellite image of the test site taken from Google Earth. The ground at and around the microphones and aircraft consists of either concrete, asphalt, or packed earth with limited and scattered brush and grass.

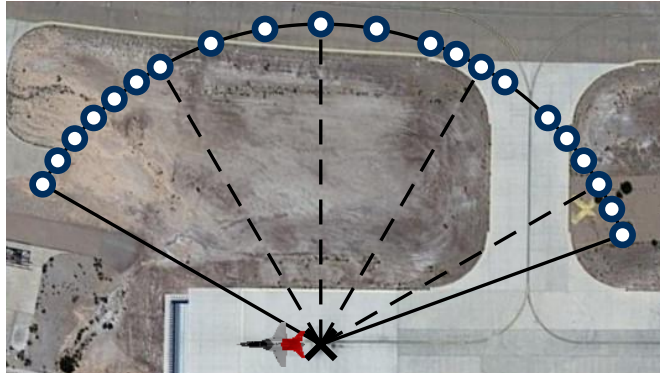


Figure 2: Approximate locations of the 76 m microphones, superimposed on a Google Earth satellite image of the test site.

3. ANALYSIS

A. MOTIVATION

The autospectral densities measured at AB at the 40°, 90°, and 150° microphones are shown in Fig. 3. Autospectral densities from jet noise measurements are typically a smooth curve, with an additional hump present in cases where broadband shock-associated noise is present. These kinds of spectra are observed in the near-field similarity spectra analysis by Epps et al.⁶ In the far-field spectra shown in Fig. 3, however, deep nulls are observed just below 1 kHz for both the 40° and 90° mics, with a less evident null at roughly the same frequency for the 150° case. These nulls, attributed to ground reflections, can be seen at each of the four considered engine conditions, as shown in the spatiospectral maps in Fig. 4. Note that in both Figs. 3 and 4, only one spectral null is present. This indicates a turbulent atmosphere, as multiple nulls would be expected for a case without turbulence³.

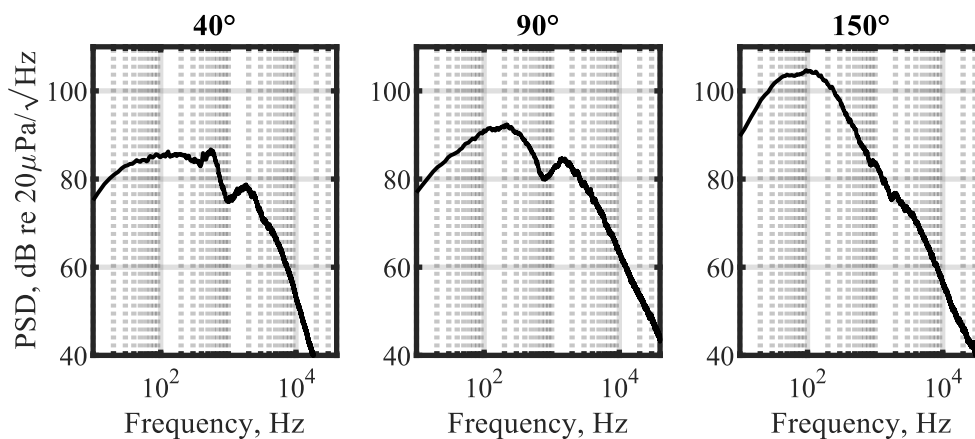


Figure 3: Autospectral densities of the 40°, 90°, and 150° microphones calculated from the raw measured data.

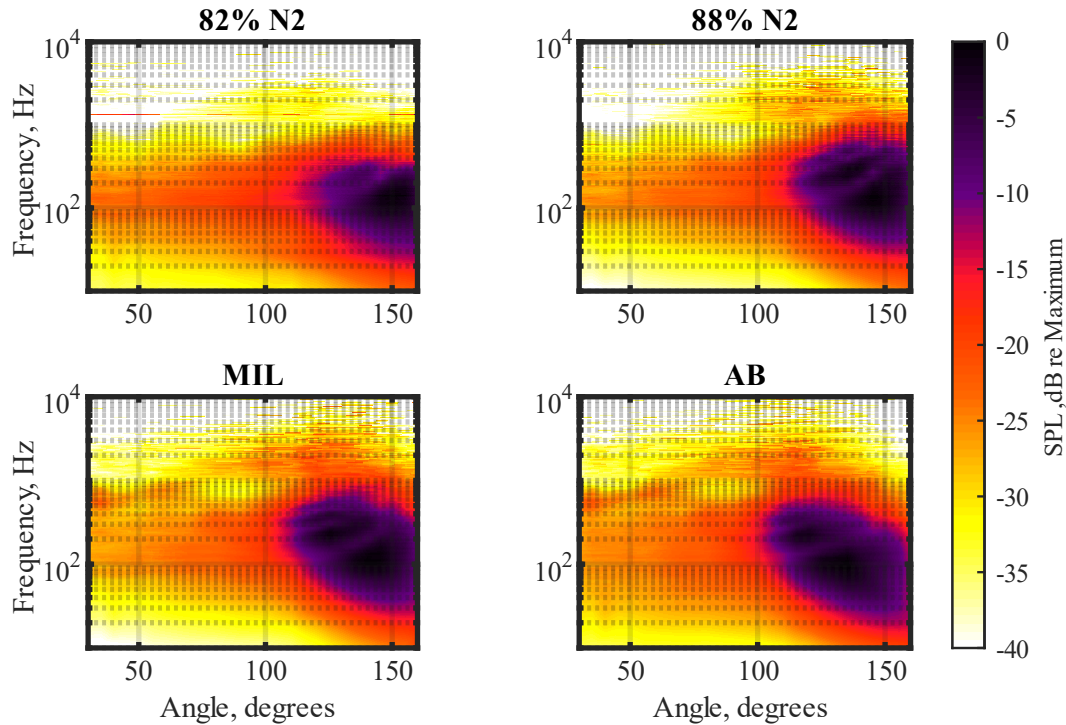


Figure 4: Spatospectral maps at each engine condition, calculated from the raw measured data.

At each engine power, the null is observed at ~ 800 Hz. This interference is particularly problematic at supersonic engine conditions, as this null occurs where broadband shock-associated noise (BSN) is dominant⁶. Because ground reflections change overall sound pressure and power levels (OASPL and OAPWL, respectively), studies that connect acoustic measurements with physical phenomena should attempt to implement some type of correction to account for this interference.

B. GROUND REFLECTION MODEL

The model used here to correct for the effects of ground reflections is given in detail in Gee et al.³. The initial framework for this model came from Daigle¹ who developed an expression for the time-averaged squared pressure from a simple source as observed by some receiver that accounts for the effects of a turbulent atmosphere and a finite impedance ground. The limitations in accounting for finite ground impedance described by Daigle are improved upon by implementing an extended-reacting ground approach, as given by Embleton et al.⁷. Gee et al.³ further improved this model by accounting for multiple sources rather than a single source. The authors provided two models, one for incoherent source interactions and another for coherent source interactions. Rather than attempting to model the complex partially correlated nature of jet noise⁸, only results from coherent and incoherent source interaction models are provided here, with the assumption that the actual jet behavior will be bounded by these two extreme cases.

The parameters needed to run the model are the geometric positions of the sources and receiver, the mean-square fluctuating index of refraction, $\langle \mu^2 \rangle$, the effective turbulence length scale, L , and the effective flow resistivity, σ . Figure 5 shows the source and receiver geometries used for this study. A uniform line source made up of 20 simple sources which began at the MARP and continued downstream for 2 m (roughly 3 nozzle exit diameters at AB⁹) was implemented into the model. Unfortunately, significant numerical errors were present if the receiver was located at any position other than 90° . To avoid this, it was assumed that the results from the 90° source position approximated the effects of ground reflections and atmospheric turbulence at all angles. Values for $\langle \mu^2 \rangle$ and L for different ambient conditions can be found in Johnson et al.¹⁰. The values chosen here are $\langle \mu^2 \rangle = 1 \times 10^{-5}$ and $L = 1.1$ m, both typical values for near-ground propagation. A table of σ values is given for several different ground conditions in Embleton et al.⁷. The ground near the test site primarily consisted

of packed, exposed earth, occasional gravel, and limited brush. These conditions most closely matched the “roadside dirt” description in Embleton et al., which led to the chosen value $\sigma = 700 \text{ Pa s/m}^2$.

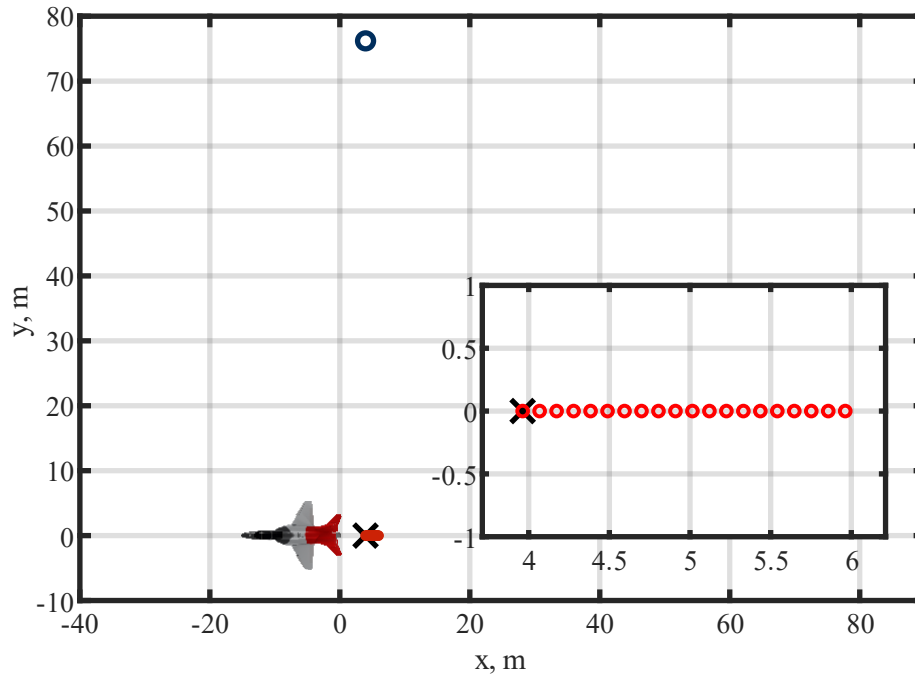


Figure 5: Diagram representing the line source and receiver geometries input into the ground reflection model. Sources are represented by red markers and the receiver by a blue marker.

Inputting these parameters yields the relative sound pressure level (SPL) spectrum shown in Fig. 6. This spectrum represents the difference between the free-field autospectrum of the line-source, and the autospectrum of the line-source after accounting for turbulence and ground reflection effects, as defined by the input parameters. Note that both the coherent and incoherent source interaction curves have a distinct null just before 1 kHz, a 6 dB decrease at low frequencies, and a roughly 2 dB decrease at higher frequencies. The difference between the two source interaction models is the depth and location of the interference null.

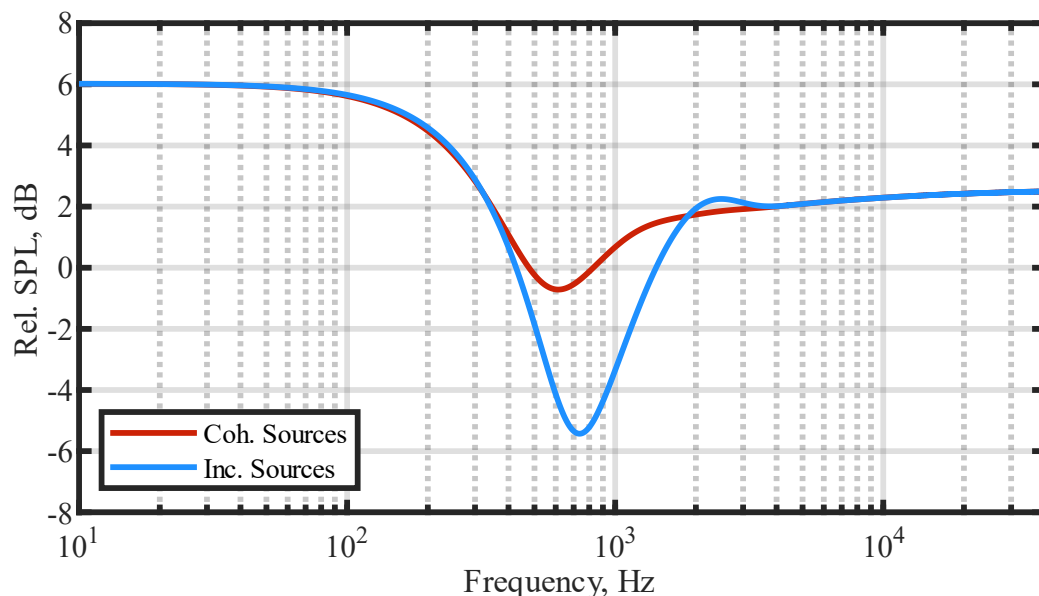


Figure 6: The relative SPL spectrum calculated from both ground reflection models.

C. MODEL IMPLEMENTATION

Figure 7 shows the same autospectral densities from Fig. 3, but also includes the resulting autospectral densities after subtracting the relative spectrum given in Fig. 5. At 40° and 90°, the incoherent source interaction model smooths the null observed in the raw data and results in an autospectral density that more closely resembles typical jet noise spectra. The corrected spectrum at 40° also shows an additional peak at ~600 Hz. This additional peak is also seen in spectra generated from the near-field upstream data from this T-7A measurement⁶ and is attributed to BSN. While the incoherent source model appears to be the most appropriate for the 40° and 90° cases, that does not appear to be the case for the downstream or 150° case. There, the coherent source model appears to most appropriately resemble the smooth curve autospectrum of jet noise, while the incoherent source model introduces a bump in the spectrum that would not be explained by jet noise theory.

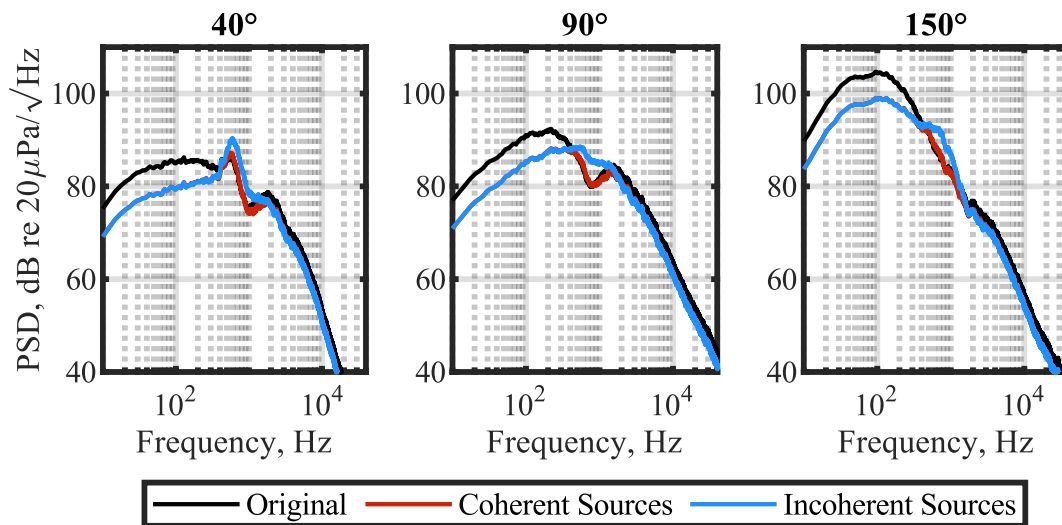


Figure 7: The raw and corrected autospectral densities of the 40°, 90°, and 150° microphones at AB.

Because no part of the model accounts for any changes in engine power, it is appropriate to use the same correction at each engine condition. This is shown in Fig. 8, where the same correction is applied to data measured at the 40°, 90°, and 150° microphones at each of the evaluated engine conditions. Note that the interference null occurs at roughly the same frequency for each engine condition and the implemented correction appears to appropriately correct the spectra in each case.

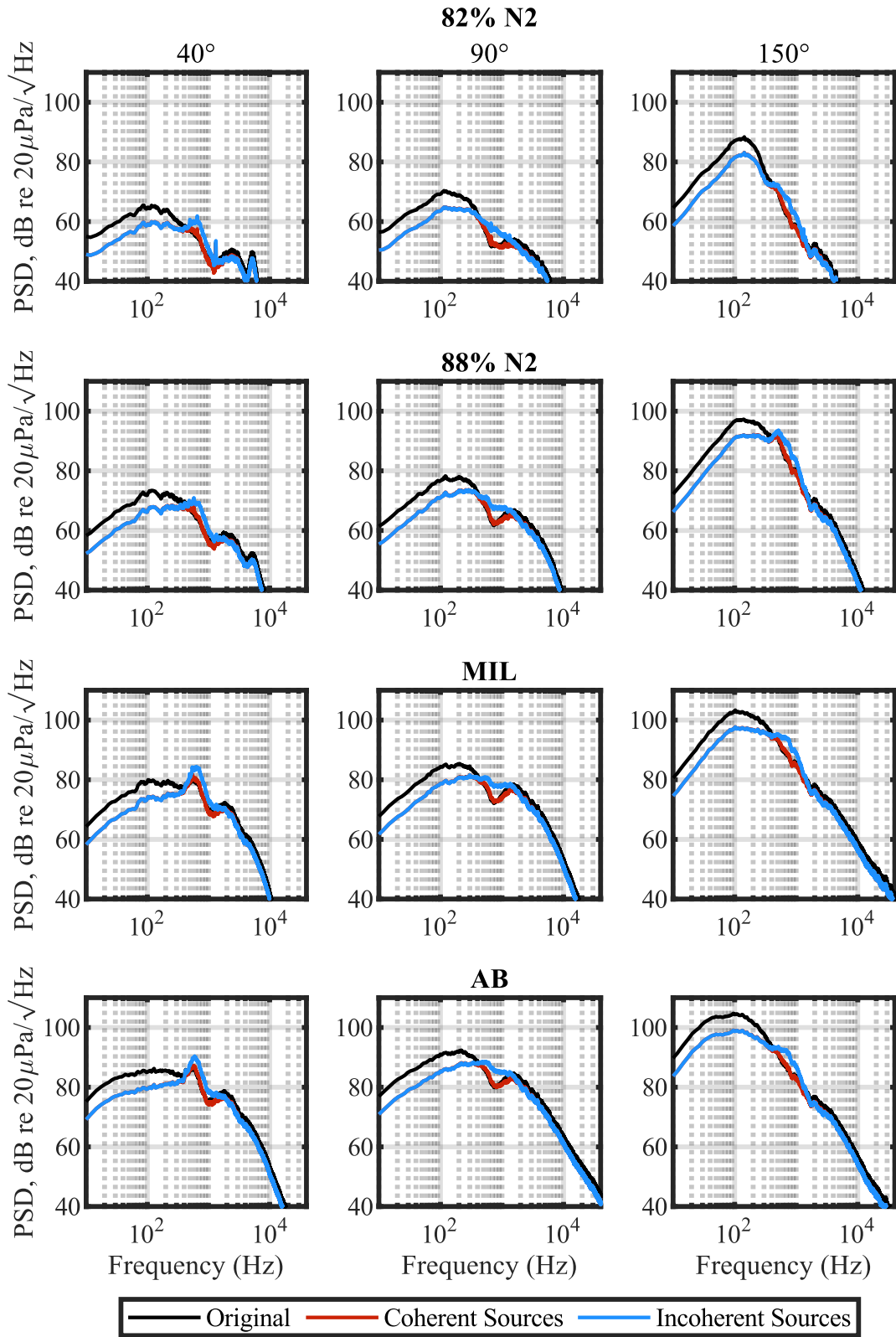


Figure 8: Original and ground reflection-corrected autospectral densities at 40°, 90°, and 150° at each engine condition.

Figure 9 shows spatio-spectral maps for each engine condition from Fig. 4 after implementing the ground reflection model. The correction used here is the decibel averaged value of the coherent and incoherent source models. Note the interference nulls, while still present, are significantly less apparent. Additionally, the upstream angles at both MIL and AB now show more apparent signs of BSN.

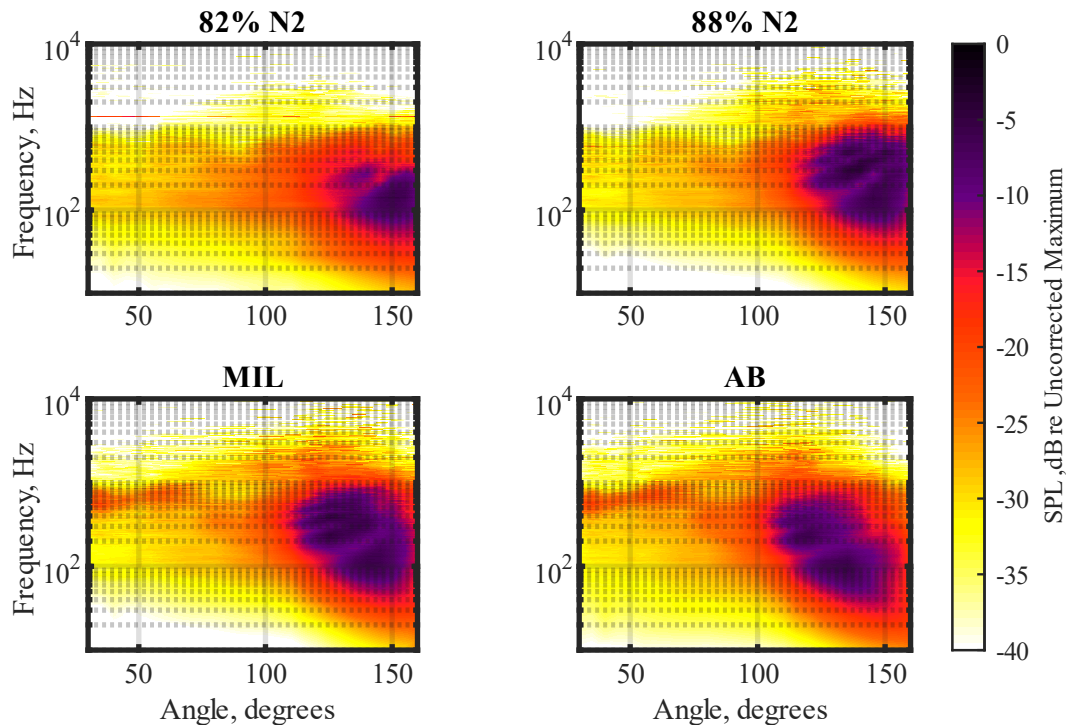


Figure 9: Ground reflection-corrected spatio-spectral maps at each engine condition. Values are plotted relative to the raw maximum value for each engine condition.

Finally, Fig. 10 shows how the different ground reflection source models affected the OASPL at different angles. Note the change in OASPL is not uniform across angles or engine conditions. Ground reflection interference does not yield a simple 3 dB reduction but is rather much more complicated. In some cases, such as the upstream angles of MIL and AB, there is even an increase in OASPL at upstream angles at the supersonic conditions after accounting for ground reflections, likely from the increased BSN peak.

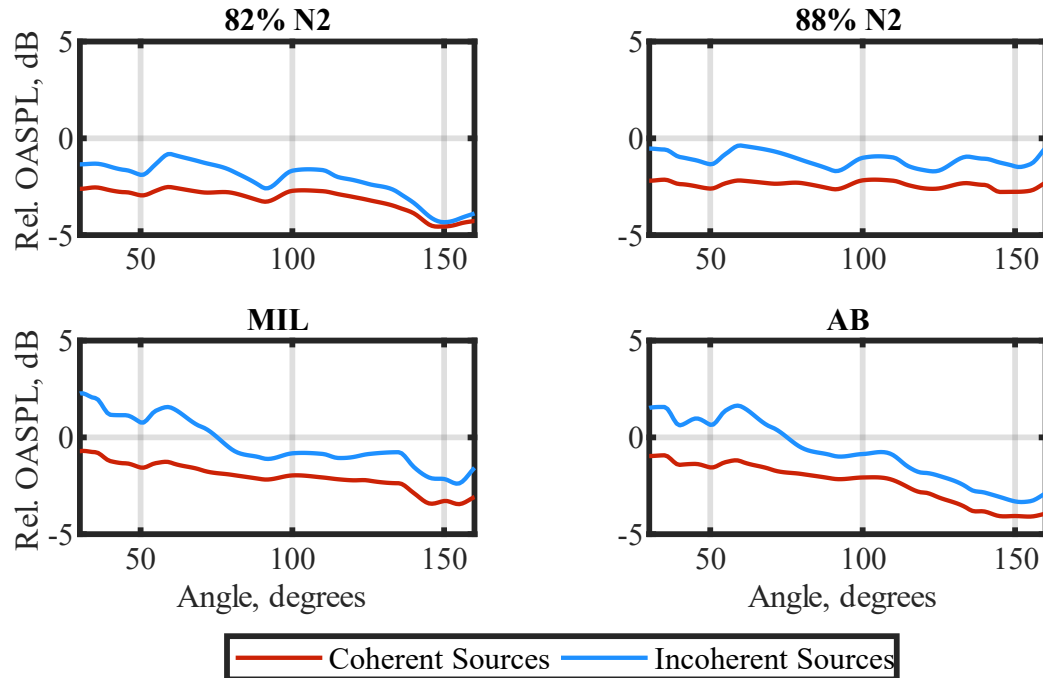


Figure 10: Effects of the ground reflection models on the OASPL across all angles and at each engine condition.

4. CONCLUSION

Ground reflection and turbulence effects pose unique challenges in the acoustic far-field for outdoor noise measurements of full-scale tactical aircraft. From a recent T-7A-installed GE F404 engine measurement, interference nulls, attributed to ground reflections, were observed in the autospectral densities measured in the far-field at or near the peak frequency. A model developed by Gee et al.³ to correct ground reflection effects in rocket noise measurements was implemented into the T-7A far-field data. This model accounts for finite ground impedance, atmospheric turbulence, and an extended source treated as an array of coherent and incoherent monopoles. Comparing the corrected spectra with near-field spectra⁶ show that the incoherent source model is most appropriate at upstream and sideline angles, while the coherent source model works better at downstream angles. Though imperfect, this model sufficiently corrects the spectra to resemble jet noise spectra more closely and represents an important first step in accounting for the effects of ground reflections.

ACKNOWLEDGMENTS

The authors gratefully acknowledge the funding provided by the Office of Naval Research under grant number N00014-21-1-2069 with project monitor Dr. Steven Martens, Code 351 Jet Noise Reduction. Measurements were funded through the Advanced Pilot Training System Program Office and the Air Force Research Laboratory. Distribution A. Approved for public release; distribution unlimited.

REFERENCES

- (1) Daigle, G. A. Effects of Atmospheric Turbulence on the Interference of Sound Waves above a Finite Impedance Boundary. *J. Acoust. Soc. Am.* **1979**, 65 (1), 45–49.
- (2) Salomons, E. M.; Ostashev, V. E.; Clifford, S. F.; Lataitis, R. J. Sound Propagation in a Turbulent Atmosphere near the Ground: An Approach Based on the Spectral Representation of Refractive-Index Fluctuations. *J. Acoust. Soc. Am.* **2001**, 109 (5), 1881–1893.
- (3) Gee, K. L.; Neilsen, T. B.; James, M. M. Including Source Correlation and Atmospheric Turbulence in a Ground Reflection Model for Rocket Noise. *Proc. Mtgs. Acoust.* **2014**, 22.
- (4) Christian, M. A.; Gee, K. L.; Streeter, J. B.; Mathews, L. T.; Wall, A. T.; Johnson, J. P.; Campbell, S. C. Installed F404 Noise Radiation Characteristics from Far-Field Measurements. *AIAA Paper 2022-3027* **2022**.

-
- (5) Leete, K. M.; Vaughn, A. B.; Bassett, M. S.; Rasband, R. D.; Novakovich, D. J.; Gee, K. L.; Campbell, S. C.; Mobley, F. S.; Wall, A. T. Jet Noise Measurements of an Installed GE F404 Engine. *AIAA Paper 2021-1638* **2021**.
 - (6) Epps, K. A.; Merrill, C. D.; Vaughn, A. B.; Leete, K. M.; Gee, K. L.; Wall, A. T. Preliminary Similarity Spectra Analysis of Noise from a High-Performance Trainer Aircraft. *Proc. Mtgs. Acoust.* **2020**, *42*.
 - (7) Embleton, T. F. W.; Piercy, J. E.; Daigle, G. A. Effective Flow Resistivity of Ground Surfaces Determined by Acoustical Measurements. *J. Acoust. Soc. Am.* **1983**, *74* (4), 1239–1244.
 - (8) Tam, C. K. W.; Golebiowski, M.; Seiner, J. M. On the Two Components of Turbulent Mixing Noise from Supersonic Jets. *AIAA Paper 96-1716* **1996**.
 - (9) Mathews, L. T.; Gee, K. L.; Leete, K. M.; Wall, A. T. Acoustic Source Characterization of an Installed GE F404 Engine Using Near-Field Acoustical Holography. *AIAA Paper 2022-3028* **2022**.
 - (10) Johnson, M. A.; Raspet, R.; Bobak, M. T. A Turbulence Model for Sound Propagation from an Elevated Source above Level Ground. *J. Acoust. Soc. Am.* **1987**, *81* (3), 638–646.